

## RESEARCH ARTICLE

# Actin-capping proteins play essential roles in the asymmetric division of maturing mouse oocytes

Yu-Jin Jo, Woo-In Jang, Suk Namgoong\* and Nam-Hyung Kim\*

## ABSTRACT

Actin polymerization is essential for various stages of mammalian oocyte maturation, including spindle migration, actin cap formation, polar body extrusion and cytokinesis. The heterodimeric actin-capping protein is an essential element of the actin cytoskeleton. It binds to the fast-growing (barbed) ends of actin filaments and plays essential roles in various actin-mediated cellular processes. However, the roles of capping protein in mammalian oocyte maturation are poorly understood. We investigated the roles of capping protein in mouse oocytes and found that it is essential for correct asymmetric spindle migration and polar body extrusion. Capping protein mainly localized in the cytoplasm during maturation. By knocking down or ectopically overexpressing this protein, we revealed that it is crucial for efficient spindle migration and maintenance of the cytoplasmic actin mesh density. Expression of the capping-protein-binding region of CARMIL (also known as LRRC16A) impaired spindle migration and polar body extrusion during oocyte maturation and decreased the density of the cytoplasmic actin mesh. Taken together, these findings show that capping protein is an essential component of the actin cytoskeleton machinery that plays crucial roles in oocyte maturation, presumably by controlling the cytoplasmic actin mesh density.

**KEY WORDS:** Actin, Capping protein, Maturation, Oocyte

## INTRODUCTION

Dynamic microfilament reorganization is essential for various stages of mammalian oocyte maturation, including asymmetric spindle migration, cortical actin cap formation, polar body extrusion and cytokinesis (Almonacid et al., 2014; Li and Albertini, 2013; Sun and Schatten, 2006; Yi and Li, 2012). During the dynamic reorganization of microfilaments, actin filament formation, elongation and depolymerization are tightly regulated by various actin-binding proteins (Pollard and Borisy, 2003; Pollard and Cooper, 2009). Actin nucleators initiate new actin filaments (Firat-Karalar and Welch, 2011), and several of these proteins are essential for oocyte maturation, including formin-2 (FMN2) (Dumont et al., 2007; Leader et al., 2002), Spire (Pfender et al., 2011) and the Arp2/3 complex (Chaigne et al., 2013; Sun et al., 2011b; Yi et al., 2011). Various nucleation-promoting factors, including JMY (Sun et al., 2011a), N-WASP (Yi et al., 2011) and WAVE2 (Chaigne et al., 2013; Sun

et al., 2011c), activate the Arp2/3 complex and help to form new branched actin filaments. In addition to actin nucleators, other actin-binding proteins cap, depolymerize, elongate and bundle actin filaments, and are therefore crucial for actin dynamics in various cell types (Pollard and Cooper, 2009). For example, using purified actin-binding proteins and a bacterial actin-based motility system, Loisel et al. demonstrated that, in addition to actin and the activated Arp2/3 complex, actin-capping protein (encoded by the *Capza* and *Capzb* genes) (Cooper and Sept, 2008) and actin depolymerization factors (ADF/cofilin) (Bamburg and Bernstein, 2010) are required for motility, (Loisel et al., 1999). This indicates the importance of various actin-binding proteins in Arp2/3-mediated actin reorganization.

Capping protein is an actin-binding protein that binds to the fast-growing (barbed) ends of actin filaments with very high affinity (Caldwell et al., 1989; Cooper and Pollard, 1985; Cooper and Sept, 2008; Schafer et al., 1996). Capping protein thereby blocks the addition of actin monomers to filament ends and effectively terminates filament elongation. It is a highly conserved protein that is found from yeast to humans, and it is a heterodimer composed of two unrelated subunits,  $\alpha$  and  $\beta$  (Wear and Cooper, 2004). Various lines of biochemical evidence (Akin and Mullins, 2008; Loisel et al., 1999) and cellular experiments (Fan et al., 2011; Mejillano et al., 2004; Pappas et al., 2008) have shown that capping protein is essential for various actin-mediated processes. For example, knockdown of capping protein in fast-moving fish keratinocytes causes filopodia-like structures to appear at cell edges (Mejillano et al., 2004), indicating the importance of this protein in cell migration. In addition, the knockdown of capping protein in hippocampal neurons impairs dendritic spine formation and alters the morphology of dendritic spines (Fan et al., 2011). In striated muscle, knockdown of capping protein perturbs the uniform alignment of the barbed ends of actin filaments (Pappas et al., 2008). These results highlight the importance and varied functions of this protein in the formation of actin-based structures and in actin filament dynamics.

Capping protein plays crucial roles in dynamic actin polymerization, especially Arp2/3-mediated actin polymerization. Therefore, the termination of actin elongation by capping protein is hypothesized to play essential roles in Arp2/3-driven actin polymerization during oocyte maturation. However, the roles of capping protein in oocyte maturation and the preimplantation development of embryos are poorly understood. In this study, we investigated the roles of capping protein at various stages of mouse oocyte maturation. Using RNA interference (RNAi)-mediated knockdown of *CapZ $\alpha$*  and *CapZ $\beta$* , ectopic expression of capping protein and expression of capping-protein-binding region of the CARMIL protein that inhibits this protein (Yang et al., 2005), we showed that capping protein plays essential roles in asymmetric spindle migration and extrusion of the first polar body.

Department of Animal Sciences, Chungbuk National University, Cheong-Ju, ChungChungBuk-do, 361-763, Republic of Korea.

\*Authors for correspondence (suknamgoong@chungbuk.ac.kr; nhkim@chungbuk.ac.kr)

Received 22 September 2014; Accepted 7 November 2014

## RESULTS

### Presence of capping protein in the oocyte cytoplasm during oocyte maturation

There were no reports on capping protein expression in mammalian oocytes. Therefore, we examined the expression of capping protein at the mRNA and protein levels using quantitative reverse-transcription PCR and western blotting, respectively. *Capza1* and *Capzb2* mRNAs (the product of the *Capza1* gene and an isoform of the *Capzb* gene, respectively) were detected at every stage of mouse oocyte development (Fig. 1A). Using a monoclonal antibody against the  $\beta$ -tentacle region of CapZ $\beta$ 2 (Schafer et al., 1996), we investigated capping protein expression. CapZ $\beta$ 2 protein was found in both immature (germinal-vesicle stage; GV) and mature [metaphase (M) II] oocytes (Fig. 1B). The intensity of the CapZ $\beta$ 2 band was higher in MII-stage oocytes than in GV-stage oocytes. Next, we investigated the localization of capping protein in oocytes at various stages of development. At all developmental stages, capping protein was dispersed throughout the entire oocyte cytoplasm. The distribution of capping protein was similar in samples fixed with paraformaldehyde (Fig. 1C) and those fixed with methanol (supplementary material Fig. S1A). Furthermore, when we injected complementary (c)RNA encoding human GFP–CapZ $\beta$ 2 and GFP–CapZ $\alpha$ 1 into oocytes, the GFP signal was dispersed throughout the entire cytoplasm, similar to the immunostaining results (supplementary material Fig. S1B). Although the distribution of cortical actin changed dramatically during oocyte maturation, especially in the cortical actin cap region (Fig. 1C), the level of capping protein near this region did not increase. These results suggest that capping protein is mainly distributed in the oocyte cytoplasm during oocyte maturation.

### Knockdown of capping protein impairs the asymmetric division of oocytes

Considering that capping protein is involved in various Arp2/3-mediated actin polymerization processes (Fan et al., 2011;

Mejillano et al., 2004; Pappas et al., 2008), we reasoned that it might play important roles in oocyte maturation and/or polar body extrusion. To understand the roles of capping protein in spindle migration and polar body extrusion in mouse oocytes, we simultaneously injected *Capza1*- and *Capzb2*-specific double-stranded (ds)RNA to knock down the expression of both subunits of capping protein. Following this injection, mRNA levels of *Capza1* and *Capzb2* were decreased to 17% and 13% of those in control oocytes, respectively (Fig. 2A). Immunostaining showed that the protein level of CapZ $\beta$ 2 was markedly decreased after dsRNA injection (Fig. 2B). In dsRNA-injected oocytes, the fluorescence intensity of CapZ $\beta$ 2 labeling was 28% of the level in control oocytes ( $P < 0.001$ ) (Fig. 2C), indicating that dsRNA injection significantly decreased the capping protein level in oocytes.

Next, we observed the effect of capping protein knockdown on oocyte maturation. The percentage of oocytes that matured to the MII stage did not significantly differ between the control and capping-protein-knockdown groups (data not shown). However, the percentage of oocytes that underwent asymmetric division was significantly lower in the capping-protein-knockdown group than in the control group. Oocytes with knockdown of capping protein frequently exhibited an abnormally large polar body or underwent symmetric division, and the co-injection of RNAi-resistant human CapZ $\alpha$ 1 and CapZ $\beta$ 2 rescued these defects (Fig. 2D).

We measured the ratio of the polar body diameter to the diameter of the oocyte (Fig. 2E,F). The mean value of this ratio was  $0.39 \pm 0.01$  (mean  $\pm$  s.e.m.) in control oocytes. This value was significantly higher in capping-protein-knockdown oocytes ( $0.56 \pm 0.018$ ;  $P < 0.001$ ), and it did not significantly differ between the rescue and control groups ( $0.39 \pm 0.01$  versus  $0.43 \pm 0.02$ ;  $P > 0.05$ ). An abnormally large polar body was defined as that which had a diameter 50% greater than that of the oocyte. Based on this definition, 60% ( $n = 94$ ) of oocytes in the capping-protein-knockdown group, 7% ( $n = 86$ ) of oocytes in the control group and 18% ( $n = 50$ ) of oocytes in the rescue group

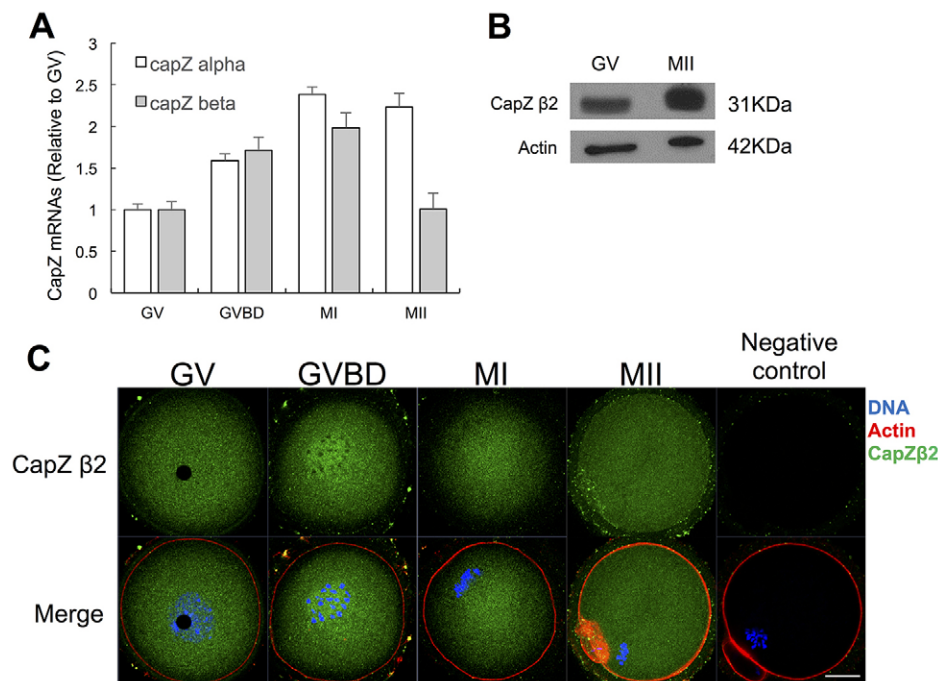


**Fig. 1. Expression and localization of actin-capping protein during mouse oocyte maturation.** (A) mRNA expression of *Capza1* (capZ alpha) and *Capzb2* (capZ beta) during mouse oocyte meiotic maturation. mRNA levels were measured by real-time reverse-transcription PCR. *Capza1* and *Capzb2* expression levels at each maturation stage are presented as relative fold changes compared with levels in GV-stage oocytes. Samples were collected at 0, 4, 8 or 12 h after the resumption of maturation, when most oocytes were at the GV, GV breakdown (GVBD), metaphase (M) I and MII stages, respectively. Data show the mean  $\pm$  s.e.m. (three independent experiments). (B) Western blot analysis of CapZ $\beta$ 2 protein levels in GV- and MII-stage oocytes. A total of 100 oocytes at GV or MII stage were used. (C) Subcellular localization of CapZ $\beta$ 2 during mouse oocyte meiotic maturation. Immunofluorescent staining was performed using an anti-CapZ $\beta$ 2 antibody. For the negative control, the anti-CapZ $\beta$ 2 primary antibody was omitted. Capping protein accumulated throughout the cytoplasm during oocyte maturation. Blue, DNA; red, actin; green, CapZ $\beta$ 2. Scale bar: 20  $\mu$ m.

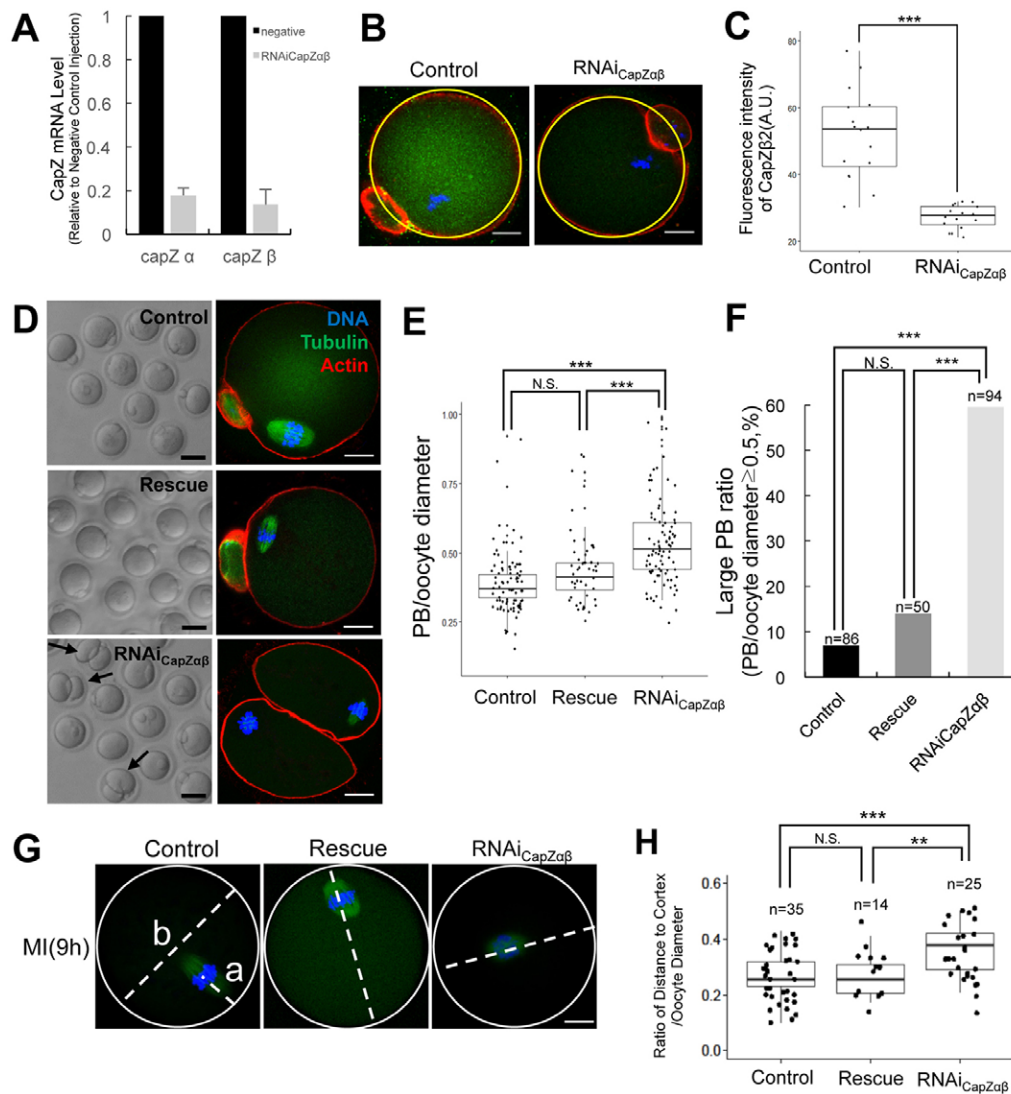


**Fig. 2. Actin-capping protein is essential for asymmetric division during oocyte maturation.** (A) Knockdown of CapZ $\alpha$ 1 and CapZ $\beta$ 2 was performed by dsRNA injection. mRNA levels of *Capza1* and *Capzb2* after dsRNA microinjection are shown. mRNA levels in dsRNA-injected oocytes ( $n=20$ ) are expressed relative to those in negative control siRNA-injected oocytes. Data indicate the mean  $\pm$  s.e.m. (three independent experiments). (B,C) Decreased protein levels of CapZ $\alpha$ 1 and CapZ $\beta$ 2 after dsRNA injection. (B) Immunostaining for CapZ $\beta$ 2 in negative control siRNA-injected (Control) and dsRNA-injected ( $\text{RNAi}_{\text{CapZ}\alpha/\beta}$ ) oocytes at the metaphase II (MII) stage. The yellow circle shows the oocyte boundary. Red, actin; green, CapZ $\beta$ 2; blue, DNA. Scale bar: 20  $\mu\text{m}$ . (C) Fluorescence intensity of CapZ $\beta$ 2 labeling after injection of *Capza1*- and *Capzb2*-specific dsRNA ( $\text{RNAi}_{\text{CapZ}\alpha/\beta}$ ). A.U. arbitrary units. \*\*\* $P<0.001$ . (D) Impairment of asymmetric division by knockdown of capping protein. After dsRNA injection and maturation arrest to ensure that capping protein was knocked down, maturation was resumed and samples were collected 12 h later. Arrows indicate abnormal polar body extrusions. Representative oocytes were immunostained for actin (red),  $\beta$ -tubulin (green) and DNA (blue). Scale bars: 50  $\mu\text{m}$  (black) and 20  $\mu\text{m}$  (white). (E) Capping protein knockdown increases polar body (PB) size. The distribution of the ratio of the diameter of the polar body to that of the oocyte in control, rescue and capping-protein-knockdown oocytes is shown. \*\*\* $P<0.001$ ; N.S., not statistically significant ( $P>0.05$ ). (F) The number of oocytes with a large polar body (diameter of the polar body greater than 50% of that of the oocyte) and a two-cell-like morphology were considered to be abnormal.  $n$  values are as indicated. \*\*\* $P<0.001$ ; N.S., not statistically significant ( $P>0.05$ ). (G) Spindle migration is impaired in oocytes with capping protein knockdown. Knockdown, control and rescue oocytes were sampled 9 h after meiotic resumption, and the locations of the spindle and DNA were confirmed by immunostaining of  $\beta$ -tubulin (green) and DNA (blue), respectively. The white circle shows the oocyte boundary. a, distance from the centroid of the spindle to the cortex; b, diameter of the oocyte. Scale bar: 20  $\mu\text{m}$ . (H) The distribution of spindle location in capping-protein-knockdown, control and rescue oocytes. Spindle location is expressed as a/b, where a is the distance between chromatin and the cortex and b is the oocyte diameter, as indicated in G.  $n$  values are as indicated. \*\*\* $P<0.001$ ; \*\* $P<0.01$ ; N.S., not statistically significant ( $P>0.05$ ). For C,E and H, boxes show the interquartile range; whiskers show 1.5 $\times$  the interquartile range; line represents the median.

were classified as having a large polar body (Fig. 2F). These results indicate that the knockdown of capping protein causes the failure of asymmetric division. The increased polar body size and asymmetric division failure in oocytes with capping protein

knockdown suggest that this protein is involved in spindle migration during oocyte maturation.

To investigate the effects of capping protein knockdown on spindle migration in more detail, we examined the position of the

spindle at 9.5 h after the resumption of oocyte maturation. The mean spindle position (distance between the spindle and the cortex divided by the oocyte diameter) was  $0.27 \pm 0.012$  ( $n=35$ ) in control oocytes and  $0.35 \pm 0.018$  ( $n=25$ ) in oocytes with knockdown of capping protein, indicating that the knockdown significantly retarded spindle migration ( $P < 0.001$ ) (Fig. 2G,H). The mean spindle position was  $0.26 \pm 0.019$  ( $n=14$ ) in the rescue group, which was not significantly different from that of the control group ( $P > 0.05$ ). These results show that capping protein is crucial for proper spindle migration during oocyte maturation (Fig. 2H).

### Knockdown of capping protein decreases the density of the cytoplasmic actin mesh

FMN2- and Spire-mediated generation of the cytoplasmic actin mesh is crucial for spindle migration (Azoury et al., 2011; Azoury et al., 2008; Dumont et al., 2007; Holubcová et al., 2013; Pfender et al., 2011). The FH2 domains of formins and capping protein bind to the same site on actin filaments; namely, the fast-growing barbed end (Cooper and Pollard, 1985; Goode and Eck, 2007; Isenberg et al., 1980; Pruyne et al., 2002; Thévenaz et al., 1998). Therefore, we hypothesized that changes in the level of capping protein in the cytoplasm would affect the cytoplasmic actin mesh. To evaluate the effects of capping protein knockdown on the level of cytoplasmic actin mesh, oocytes at MI and MII stages were stained with phalloidin, and the amount of cytoplasmic actin mesh was measured (Fig. 3A). As previously reported (Azoury et al., 2008), the level of actin mesh was higher in MI-stage oocytes than in MII-stage oocytes. When oocytes were treated with *Capza1*- and *Capzb2*-specific dsRNAs, the amount of cytoplasmic actin mesh in MI- and MII-stage oocytes was significantly decreased ( $P < 0.001$ ). Expression of RNAi-resistant human *CapZα1* and *CapZβ2* partially restored the cytoplasmic actin mesh density, especially in MII-stage oocytes ( $P > 0.05$  compared with control oocytes, Fig. 3B). These results show that the knockdown of capping protein in maturing oocytes reduces the cytoplasmic actin mesh. We also compared the cortical actin level between the control and knockdown groups (supplementary material Fig. S2). In contrast to the cytoplasmic actin mesh, the level of cortical actin did not significantly differ between the capping-protein-knockdown and control groups ( $P > 0.05$ ), and the cortical actin cap formed normally in oocytes with capping protein knockdown when the spindle approached the cortex.

### Overexpression of capping protein causes severe abnormalities in polar body extrusion

Next, we tested the effects of ectopic overexpression of capping protein on spindle migration and oocyte maturation. To overexpress capping protein, cRNA encoding GFP-fused mouse *CapZβ2* was injected into GV-stage oocytes. Whereas GFP cRNA-injected control oocytes showed no morphological defects, oocytes injected with GFP–*CapZβ2* cRNA displayed severe abnormalities in polar body formation (Fig. 4A). Although there was no relationship between polar body size and GFP intensity in GFP cRNA-injected oocytes, there was a weak correlation ( $r=0.228$ ) between GFP intensity and polar body size in GFP–*CapZβ2* cRNA-injected oocytes (supplementary material Fig. S3). Similar to the results of knockdown experiments, the percentage of oocytes that reached MII did not markedly differ between the two groups (data not shown). However, many GFP–*CapZβ2* cRNA-injected oocytes exhibited abnormalities in polar body formation. Nearly half of GFP–*CapZβ2* cRNA-injected oocytes (48%,  $n=85$ ) displayed abnormalities in polar body formation, in comparison to 12% ( $n=43$ ) of control GFP cRNA-injected oocytes ( $P < 0.001$ ,

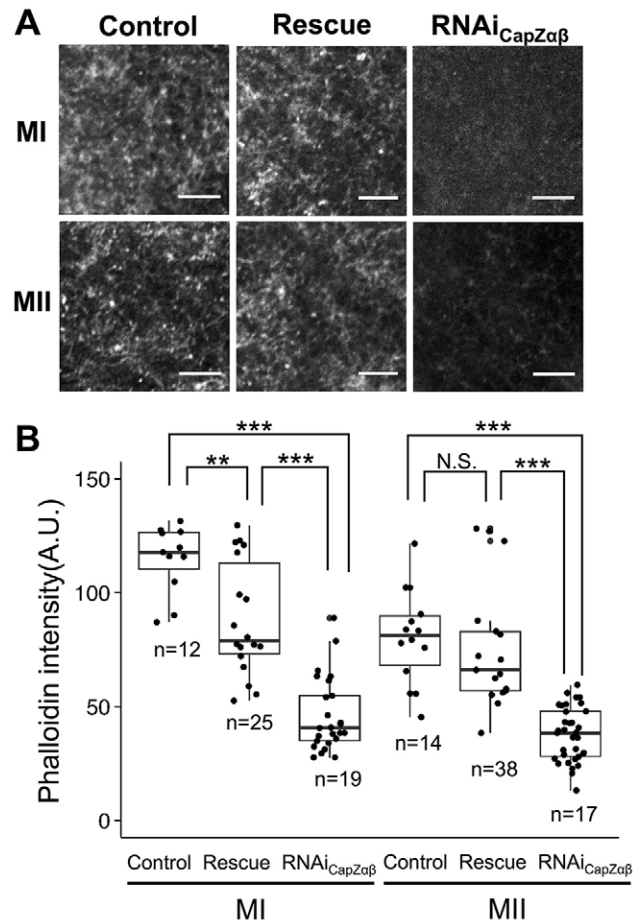


**Fig. 3. Knockdown of actin-capping protein impairs the formation of the cytoplasmic actin mesh in maturing oocytes.** (A) Phalloidin-stained cytoplasmic actin mesh in oocytes injected with negative control siRNA (Control), *Capza1*- and *Capzb2*-specific dsRNA ( $\text{RNAi}_{\text{CapZ}\alpha\beta}$ ), and cRNA encoding human *CapZα1* and *CapZβ2* (Rescue) at the MI or MII stage under the same conditions. Knockdown of capping protein impairs the formation of an appropriate amount of actin mesh. Scale bars: 3  $\mu\text{m}$ . (B) Phalloidin fluorescence intensity at 9 h (MI) and 12 h (MII) after injection of negative control siRNA (Control), *Capza1*- and *Capzb2*-specific dsRNA ( $\text{RNAi}_{\text{CapZ}\alpha\beta}$ ), and cRNA encoding human *CapZα1* and *CapZβ2* (Rescue). A.U., arbitrary units.  $n$  values are as indicated. Boxes show the interquartile range; whiskers show 1.5 $\times$  the interquartile range; line represents the median. \*\*\* $P < 0.001$ ; \*\* $P < 0.01$ ; N.S., not statistically significant.

Fig. 4B). Some of these oocytes exhibited multiple polar body-like structures or polar bodies that had flat sides, whereas others exhibited symmetric division (Fig. 4C). Similar to the distribution of endogenous capping protein, GFP–*CapZβ2* was dispersed evenly throughout the oocyte and polar body, indicating that the protein was mainly localized in the oocyte cytoplasm. Next, the level of cytoplasmic actin mesh was measured (Fig. 4D). When oocytes were treated with GFP–*CapZβ2* cRNA, the amount of actin mesh at MI and MII stages was not significantly decreased ( $P=0.93$  and  $P=0.99$ , respectively) compared with that in GFP cRNA-injected control oocytes (Fig. 4E).

### Knockdown or overexpression of capping protein affects spindle migration speed or cytokinesis timing

We performed time-lapse microscopy to investigate the effects of capping protein knockdown or ectopic overexpression on spindle migration and polar body extrusion. In control oocytes injected

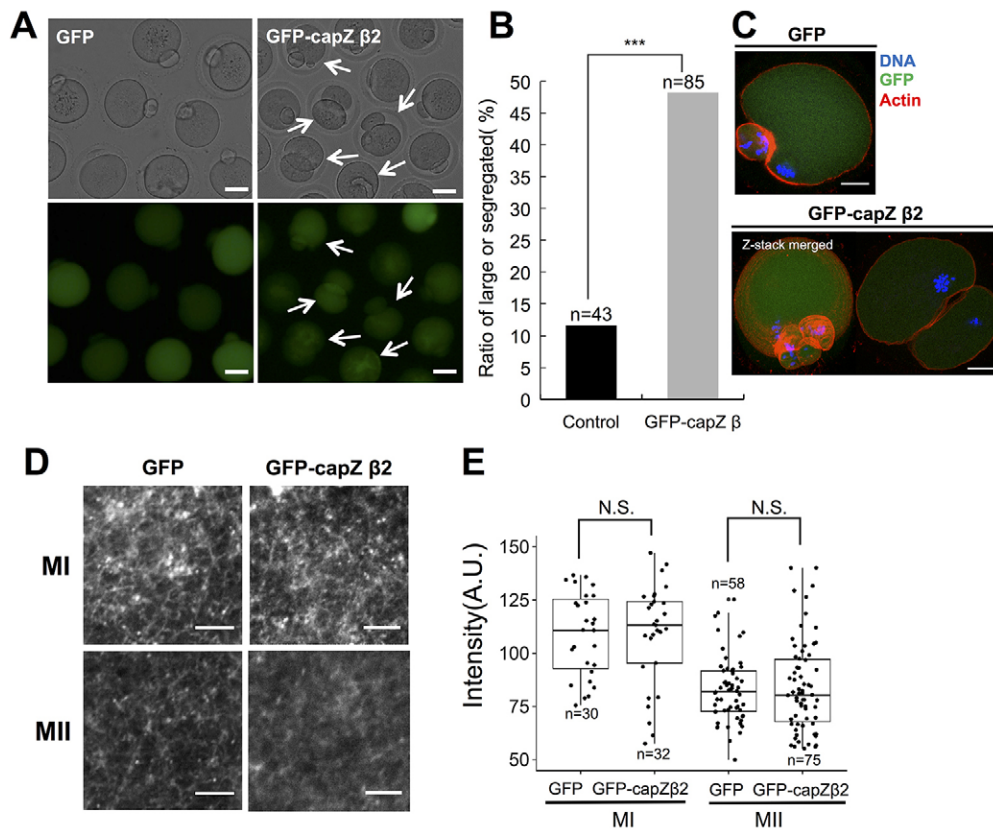


**Fig. 4. Ectopic overexpression of actin-capping protein impairs asymmetric division and causes abnormal polar body formation.** (A) Overexpression of GFP–CapZβ2 impairs asymmetric division. cRNA encoding GFP or GFP–CapZβ2 was injected into GV-stage oocytes and maturation was resumed. Whereas most GFP-injected oocytes matured and formed a normal polar body, GFP–CapZβ2-expressing oocytes frequently divided symmetrically or exhibited multiple segregation. Arrows indicate abnormal oocytes. Scale bars: 50 μm. (B) Expression of GFP–CapZβ2 increases the percentage of oocytes with a large polar body. Abnormal oocytes were defined as those in which the diameter of the polar body was greater than 50% of that of the oocyte. *n* values are as indicated. \*\*\**P*<0.001. (C) Phalloidin staining of cortical actin in control and GFP–CapZβ2-expressing oocytes. Blue, DNA; red, actin; green, GFP–CapZβ2 or GFP. Scale bars: 20 μm. (D) Actin mesh in oocytes injected with control GFP mRNA or mRNA encoding GFP–CapZβ2 at MI or MII under the same conditions. The level of actin mesh was similar in capping-protein-overexpressing oocytes and control oocytes. Scale bars: 3 μm. (E) Fluorescence intensity of actin mesh staining at 9 and 12 h (MI and MII, respectively) after injection of control GFP mRNA and GFP–CapZβ2 mRNA. A.U., arbitrary units; *n* values are as indicated. Boxes show interquartile range; whiskers show 1.5× the interquartile range; line represents the median. N.S., not statistically significant (*P*>0.05).

with  $\alpha$ -tubulin-GFP cRNA, polar body extrusion occurred 8.5–11 h after the resumption of maturation, and the size and morphology of the polar body were normal (Fig. 5A; supplementary material Movies 1, 2). As previously reported (Yi et al., 2013a), the spindle migration speed dramatically increased as the spindle approached the cortex (Fig. 5B). By contrast, spindle migration was substantially retarded in oocytes with knockdown of capping protein (Fig. 5C,D; supplementary material Movies 3, 4). In some of these oocytes, the spindle did not move or moved extremely slowly, and cytokinesis had not occurred 12 h after the resumption of maturation (supplementary material Movies 5, 6). In general, spindle movement was slowed and cytokinesis was delayed in oocytes with capping protein knockdown, as determined by spindle tracking.

Symmetric division was frequently observed in oocytes injected with cRNA encoding GFP–CapZβ2 (Fig. 5E,F). Although cases of symmetric division were observed in both capping-protein-knockdown oocytes and oocytes overexpressing capping protein, the timing of cytokinesis significantly differed between these two groups. Whereas cytokinesis occurred 11–13.5 h after the resumption of maturation in capping-protein-knockdown oocytes, it occurred far earlier in oocytes overexpressing capping protein

(9–10 h after the resumption of maturation). In some cases, cytokinesis started around 9.5 h, even before the spindle reached the cortex (Fig. 5E, upper panel), which caused oocytes to divide symmetrically. In other cases, multiple polar bodies formed (Fig. 5E, lower panel). Cytokinesis started significantly earlier in oocytes overexpressing capping protein than in control oocytes (Fig. 5F,G; *P*<0.05). Collectively, these results confirm that knockdown or overexpression of capping protein impairs spindle migration and the timing of cytokinesis.

#### Expression of the capping-protein-binding region of CARMIL decreases the maturation rate and cytoplasmic actin mesh density

The CARMIL family of proteins plays crucial roles in cell motility through interactions with various cytoskeletal proteins, including the Arp2/3 complex, myosin II and capping protein (Jung et al., 2001; Kim et al., 2012; Remmert et al., 2004; Weaver et al., 2003; Yang et al., 2005). CARMIL can inhibit actin filament capping mediated by capping protein through the direct interaction between capping protein and the capping-protein-binding region (CBR) of CARMIL (Kim et al., 2012; Yang et al., 2005). The CBR corresponds to amino acids 964–1086 of CARMIL (Zwolak et al.,

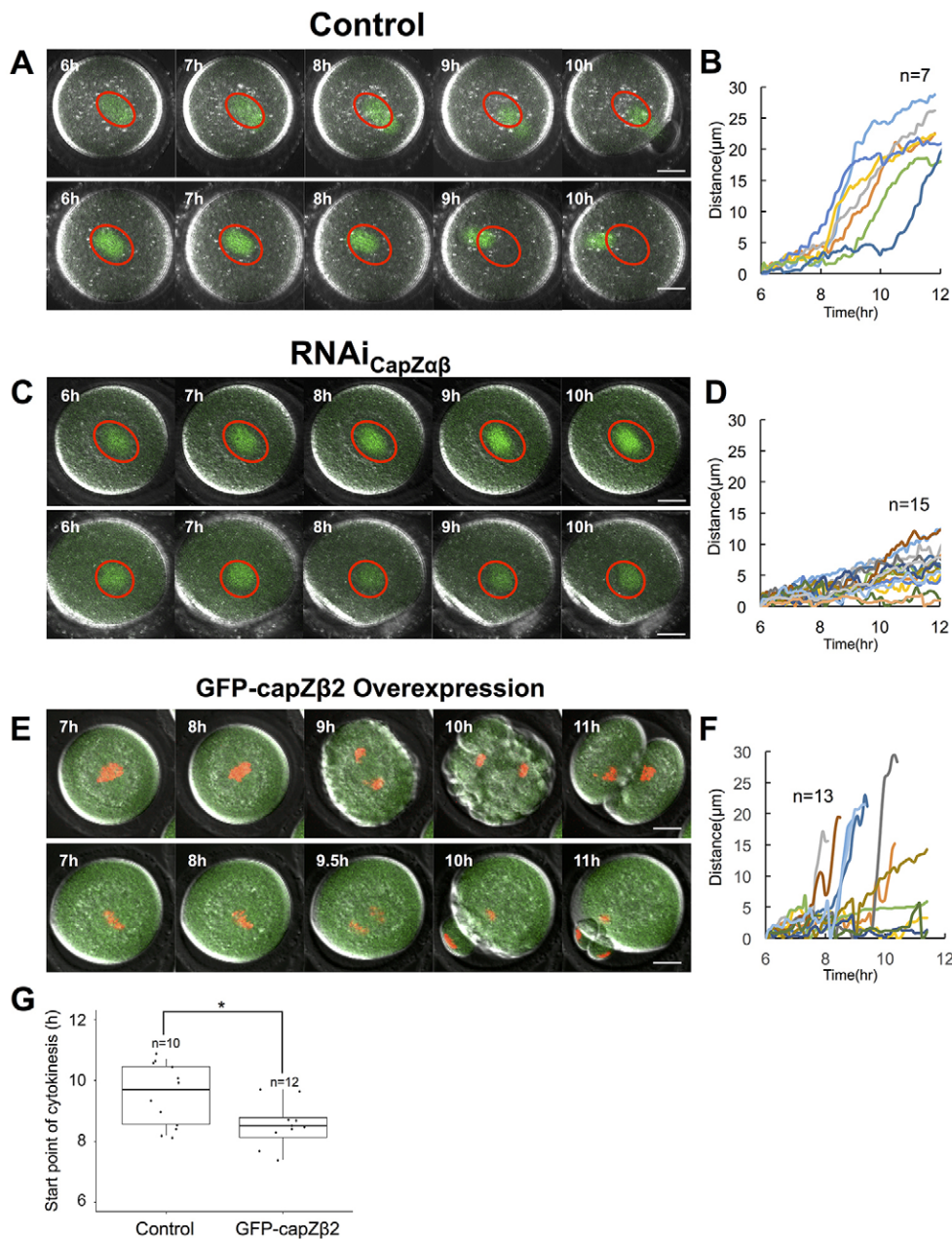


**Fig. 5. Knockdown or overexpression of actin-capping protein affects the speed of spindle migration and cytokinesis timing.** (A,C) Time-lapse microscopy of maturing control (A) and capping-protein-knockdown (C) oocytes. Spindles were visualized by injection of cRNA encoding  $\alpha$ -tubulin-GFP (green). Locations of spindles after 6 h of culture are marked with red ovals. See also supplementary material Movies 1–4. Scale bars: 20  $\mu$ m. (B,D) Tracking of spindle migration in control oocytes (B) and capping-protein-knockdown oocytes (D). The distance ( $\mu$ m) of the spindle from its starting point at each time-point is plotted. *n* values are as indicated. (E) Time-lapse microscopy of maturing oocytes overexpressing capping protein. GFP-fused capping protein was overexpressed (green), and chromatin was visualized with H2B-mCherry (red). See also supplementary material Movies 5, 6. Scale bars: 20  $\mu$ m. (F) Tracking of spindle migration in oocytes overexpressing capping protein. The distance ( $\mu$ m) of the spindle from its starting point at each time-point is plotted. (G) The time-point at which cytokinesis commenced in oocytes overexpressing capping protein. The time (h) that chromosomes began to divide is plotted. *n* values are as indicated. Boxes show interquartile range; whiskers show 1.5 $\times$  the interquartile range; line represents the median. \**P*<0.05.

2010). Expression of this region in human HT1080 cells causes similar phenotypes to those elicited by capping protein knockdown (Edwards et al., 2013), showing that the CBR of CARMIL regulates the filament capping activity of capping protein.

To provide additional evidence for the role of capping protein in oocyte maturation, we overexpressed the CBR of mouse CARMIL1 (amino acids 964–1086) fused to GFP, termed GFP-CARMIL<sub>CBR</sub>, and evaluated its effects on oocyte maturation and the density of the cytoplasmic actin mesh. The maturation rate of oocytes expressing GFP-CARMIL<sub>CBR</sub> was lower than that of control oocytes expressing GFP (*n*=98, 55% versus *n*=68, 76%; *P*<0.01; Fig. 6A). Expression of GFP-CARMIL<sub>CBR</sub> decreased the cytoplasmic actin mesh density in both MI- and MII-stage oocytes in comparison with that of GFP-injected control oocytes (Fig. 6B,C). These results indicate that negatively regulating capping protein activity by expressing the CBR of CARMIL

results in a similar phenotype to that induced by capping protein knockdown. This further confirms the essential role of this protein in oocyte maturation.

Overexpression of FMN2 or Spire1/2 can increase the density of the cytoplasmic actin mesh (Azoury et al., 2008; Holubcová et al., 2013). We tested whether CARMIL<sub>CBR</sub> can decrease the cytoplasmic actin mesh density even when the level of this mesh is abnormally high. When we overexpressed the FH1-FH2 domain of FMN2 fused to GFP, the cytoplasmic actin mesh density was significantly increased (Fig. 6D,E). However, co-expression of GFP-CARMIL<sub>CBR</sub> effectively suppressed the increased level of cytoplasmic actin mesh induced by overexpression of this FMN2 fragment (Fig. 6D, right panel; Fig. 6E). These results further support the idea that functional capping protein is essential to maintain the level of cytoplasmic actin.

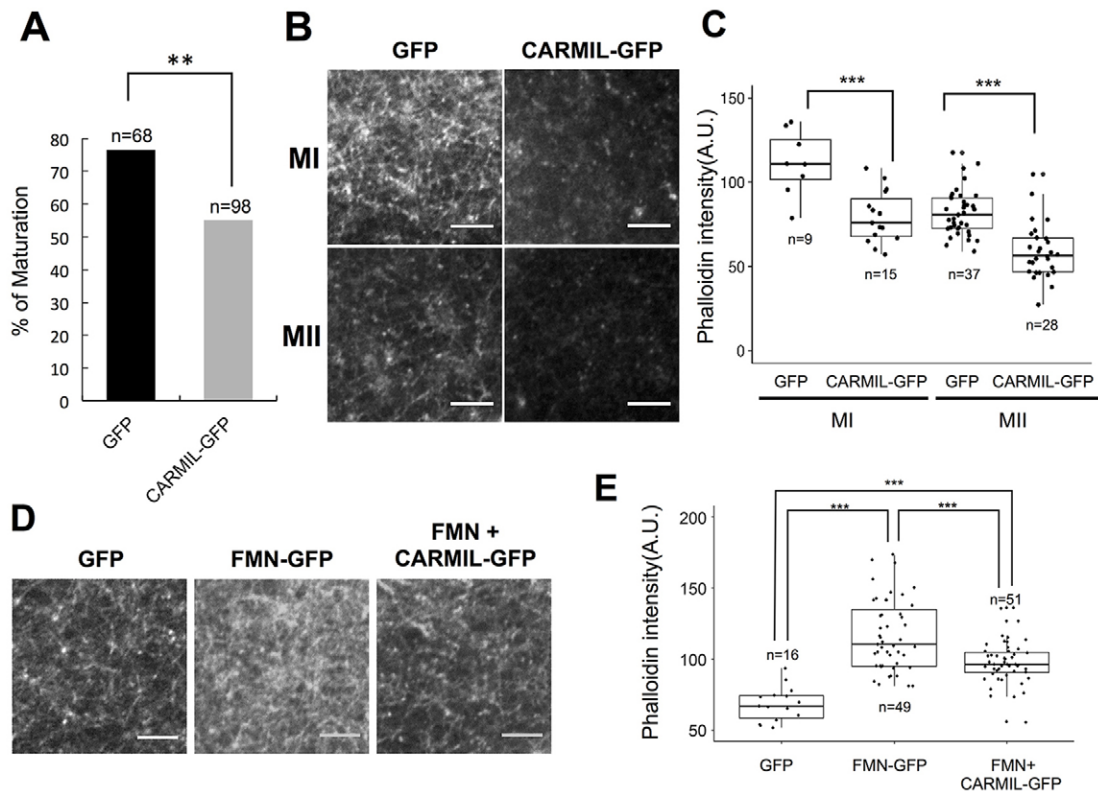


**Fig. 6. Overexpression of CARMIL affects the oocyte maturation rate and amount of cytoplasmic actin mesh.** (A) The maturation rate of oocytes expressing GFP–CARMIL<sub>CBR</sub> is lower than that of control oocytes expressing GFP. *n* values are as indicated.  $^{**}P < 0.01$ . (B) Phalloidin staining of the cytoplasmic actin mesh in oocytes injected with mRNA encoding GFP (GFP) or GFP–CARMIL<sub>CBR</sub> (CARMIL-GFP) at the MI and MII stages. Scale bars: 3  $\mu$ m. (C) Fluorescence intensity of the actin mesh at 9 and 12 h (MI and MII, respectively) after injection of mRNA encoding GFP or GFP–CARMIL<sub>CBR</sub>. A.U., arbitrary units. *n* values are as indicated.  $^{***}P < 0.001$ . (D) Effects of overexpression of FMN2 or CARMIL on the actin mesh level. Phalloidin staining of the cytoplasmic actin mesh in oocytes injected with mRNA encoding GFP (GFP), GFP–fornin alone (FMN-GFP) or GFP–fornin and GFP–CARMIL<sub>CBR</sub> (FMN+CARMIL-GFP) at the MI stage. Scale bars: 3  $\mu$ m. (E) Fluorescence intensity of the actin mesh at 9 h after injection of mRNA encoding GFP, GFP–fornin or GFP–CARMIL<sub>CBR</sub>. *n* values are as indicated.  $^{***}P < 0.001$ . For C and E, boxes show interquartile range; whiskers show 1.5 $\times$  the interquartile range; line represents the median.

## DISCUSSION

The roles of various actin nucleators in oocyte maturation have been determined recently. In addition to FMN2 (Dumont et al., 2007; Leader et al., 2002) and Spire (Pfender et al., 2011), the Arp2/3 complex and its activators, including N-WASP, WAVE2 and JMY, are involved in spindle migration and polar body extrusion (Chaigne et al., 2013; Sun et al., 2011a; Sun et al., 2013; Sun et al., 2011c; Yi et al., 2013b; Yi et al., 2011). However, the roles of other actin-binding proteins in the regulation of actin filament formation during oocyte maturation are generally unknown. In this study, we showed that capping protein is essential for the regulation of actin filament reorganization during oocyte maturation.

An intriguing observation of this study is that capping protein did not necessarily localize in actin-rich regions of oocytes. The cortical actin cap, which forms near to the approaching spindle, contains a dense actin network (Yi and Li, 2012; Yi et al., 2013a), and its formation is dependent on the Arp2/3 complex, Rho family GTPases and various nucleation-promoting factors (Dehapiot et al., 2013; Deng et al., 2007; Leblanc et al., 2011; Wang et al., 2013). Capping protein is an essential factor in an Arp2/3-mediated actin polymerization and depolymerization model called the ‘dendritic treadmilling model’ (Blanchoin et al., 2000a; Blanchoin et al., 2000b; Pollard and Borisy, 2003); therefore, this difference between the localization of

capping protein and that of the actin-rich cortical cap is unexpected. Capping protein was primarily found in the oocyte cytoplasm at all developmental stages (Fig. 1), which is where the cytoplasmic actin mesh is located (Azoury et al., 2011; Azoury et al., 2008). Changes in the level of capping protein caused abnormalities in the rate of spindle migration or in the timing of cytokinesis. Knockdown of capping protein impaired spindle migration (Fig. 2; Fig. 5C,D), whereas ectopic overexpression of capping protein increased the speed of cytokinesis (Fig. 5E,F). Interestingly, knockdown of capping protein markedly decreased the cytoplasmic actin mesh density in MI- and MII-stage oocytes (Fig. 3). How does knockdown of capping protein affect spindle migration and asymmetric division? Capping protein mainly localizes in the oocyte cytoplasm (Fig. 1). The location and roles of cytoplasmic actin mesh formation in spindle migration and asymmetric cell division have been studied previously (Azoury et al., 2011; Azoury et al., 2008; Dumont et al., 2007). Vesicle-localized FMN2 and Spire are crucial for the formation of the cytoplasmic actin mesh (Holubcová et al., 2013; Pfender et al., 2011), indicating that capping protein modulates the cytoplasmic actin mesh. Capping protein and the FH2 domain of formins bind to the barbed ends of actin filaments (Cooper and Sept, 2008). Capping protein binds to these ends tightly and thereby blocks further actin filament elongation, whereas formins bind to these ends loosely and move

as actin filaments grow (Goode and Eck, 2007). Therefore, capping protein can act as an antagonist of formin-mediated actin filament elongation (Goode and Eck, 2007; Kovar et al., 2003; Pruyne et al., 2002; Zigmond et al., 2003). Knockdown of capping protein negatively affected the density of the cytoplasmic actin mesh, whereas its overexpression did not; however, it is unclear why this is the case. One possibility is that capping protein stops the elongation of actin filaments by FMN2 and releases FMN2 from growing actin filaments. Released FMN2 could participate in a new cycle of actin filament nucleation, which would eventually lead to the formation of a dense actin mesh, as illustrated in Fig. 7. Interestingly, an *in vitro* study using fission yeast capping protein and formin Cdc12p showed that these proteins have an additive effect on the level of actin polymerization (Kovar et al., 2003), which is similar to our results regarding the cytoplasmic actin mesh. However, the detailed mechanisms underlying the interactions between capping protein and FMN2 and their relationship to the maintenance of the cytoplasmic actin mesh in oocytes need to be investigated further.

It is uncertain whether a decreased cytoplasmic actin mesh density solely underlies the failure of oocytes to divide asymmetrically when capping protein is knocked down. In addition to the cortical actin cap, actin filaments in the inner cortex region, called the subcortex, are generated by Arp2/3-mediated actin polymerization (Chaigne et al., 2013). Given that the formation of this region is crucial for asymmetric spindle migration and has a tight relationship with capping protein and Arp2/3-mediated actin polymerization, capping protein might

play a role in subcortex formation. However, considering the localization of capping protein during oocyte maturation and the increased subcortex depth during oocyte maturation, it is difficult to judge the involvement of capping protein in the regulation of Arp2/3-mediated generation of the subcortex.

Considering the roles of capping protein in oocyte maturation revealed in this study, the capping activity of this protein should also be regulated. Several actin-binding proteins regulate or compete with each other. For example, members of the CARMIL protein family have uncapping activities, and knockdown of CARMIL in somatic cells induces a similar phenotype to that caused by capping protein overexpression (Yang et al., 2005). However, the roles of CARMIL in oocyte maturation remain to be investigated. In addition to CARMIL, members of the Ena/VASP protein family, including Mena, Evl and VASP, which promote actin elongation and prevent binding of capping protein (Bear and Gertler, 2009; Bear et al., 2002), might play roles in oocyte maturation, particularly in cortical actin cap formation. However, their involvement in oocyte maturation needs to be investigated.

The current study sheds light on the roles of capping protein in oocyte maturation, especially in the regulation of the cytoplasmic actin mesh during oocyte maturation. Further studies are needed to clarify the mechanisms by which this protein modulates the density of the cytoplasmic actin mesh and to determine the possible involvement of other actin regulators in oocyte maturation, including regulators of capping protein such as CARMIL, pointed-end capping proteins such as tropomodulin and/or Ena/VASP family proteins.

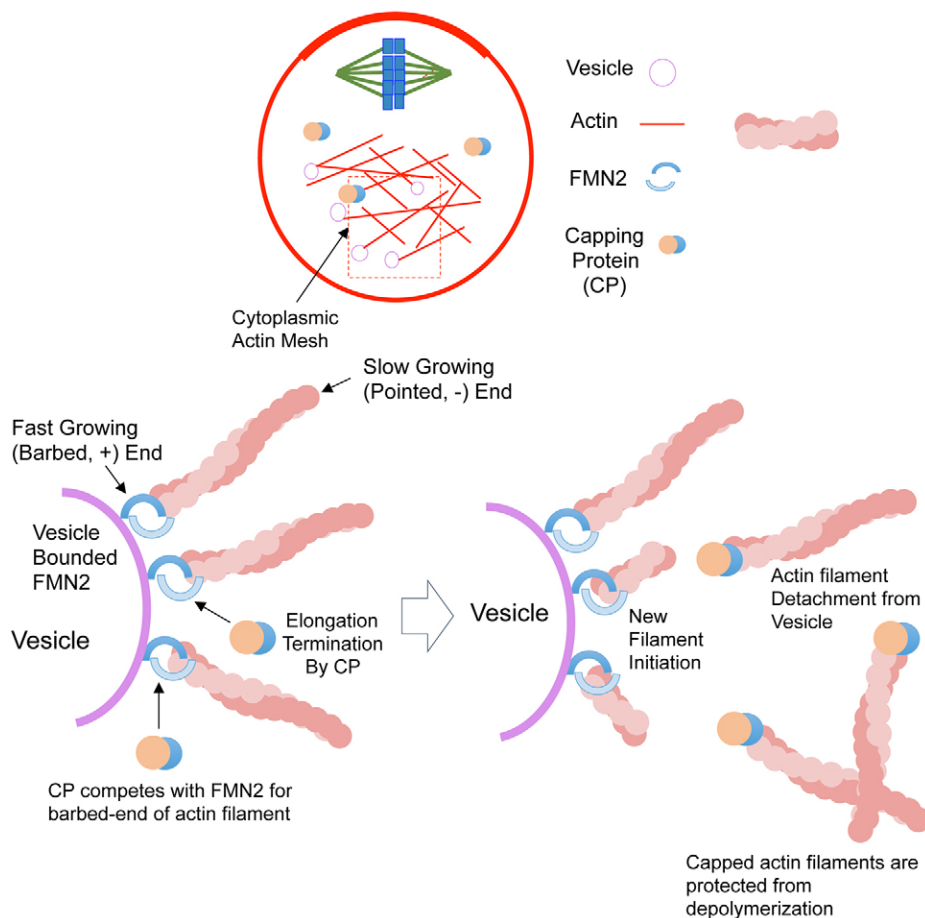


**Fig. 7. Hypothetical model for the roles of actin-capping protein in the cytoplasmic actin mesh.** The formation of the cytoplasmic actin mesh is crucial for spindle migration, and is mediated by formin-2 (FMN2) and Spire (Azoury et al., 2011; Azoury et al., 2008; Pfender et al., 2011) localized on vesicles (Holubcová et al., 2013). Capping protein (CP) binds to the fast-growing barbed ends of actin filaments and thereby blocks further actin filament elongation. Therefore, capping protein can compete with the FH2 domain of FMN2 and possibly prevent filament elongation by FMN2. The released FMN2 could initiate a new filament nucleation-elongation cycle. In addition, capping of the barbed ends of preformed filaments can protect actin filaments from depolymerization, thereby increasing the half-life of the actin mesh.



## MATERIALS AND METHODS

### Antibodies

A mouse monoclonal antibody against chicken CapZ $\beta$ 2 (3F2.3) (Schafer et al., 1996) was obtained from the Developmental Study Hybridoma Bank at the University of Iowa (Des Moines, IA), a mouse monoclonal anti- $\alpha$ -tubulin-FITC antibody was obtained from Sigma (St Louis, MO), and an Alexa-Fluor-488-conjugated goat anti-mouse-IgG antibody was purchased from Invitrogen (Carlsbad, CA).

### Oocyte collection and culture

Germinal vesicle (GV)-intact oocytes were collected from the ovaries of 6–8-week-old imprinting control region (ICR) mice and cultured in M16 medium (Sigma) under paraffin oil at 37°C in 5% CO<sub>2</sub>. Oocytes were collected for immunostaining and microinjection after they had been cultured for various amounts of time.

### Real-time quantitative PCR analysis

*Capza1* and *Capzb2* expression was analyzed by real-time quantitative PCR and the  $\Delta\Delta$ CT method (Livak and Schmittgen, 2001). Total RNA was extracted from 50 oocytes using a Dynabead mRNA DIRECT™ Kit (Life Technologies, Foster City, CA). First-strand cDNA was generated using a cDNA Synthesis Kit (Takara, Kyoto, Japan) and Oligo (dT) 12–18 primers. The PCR primers used to amplify *Capza1* and *Capzb2* are listed in supplementary material Table S1. Real-time PCR was performed with SYBR Green in a final reaction volume of 20  $\mu$ l (qPCR kit, Finnzymes, Vantaa, Finland). PCR conditions were as follows: 94°C for 10 min, followed by 39 cycles of 95°C for 15 s, 60°C for 15 s and 72°C for 45 s, and a final extension of 72°C for 5 min. Finally, relative gene expression was quantified by normalization to the level of GAPDH mRNA. Experiments were conducted in triplicate.

### Preparation of dsRNA and cRNA

*Capza1* and *Capzb2* dsRNA was generated as described previously (Li et al., 2013). Briefly, 570 bp of *Capza1* (corresponding to 364–933 bp of NM\_009797.2) and 631 bp of *Capzb2* (corresponding to 268–899 bp of NM\_001271405.1) were amplified from first-strand cDNA generated from RNA extracted from MII oocytes using gene-specific primers containing the T7 promoter sequence (supplementary material Table S1). *In vitro* transcription was performed using an mMessage mMachine Kit (Life Technologies). dsRNA was treated with DNase I to remove any contaminating DNA, purified using phenol-chloroform extraction and isopropyl alcohol precipitation, and stored at –80°C until use. pEGFP-C2 containing the mouse *Capzb2* sequence (Bear et al., 2002) was obtained from Addgene (plasmid #13298, Cambridge, MA), and the sequence encoding GFP–CapZ $\beta$ 2 was subcloned into the pCR-Blunt vector (Life Technologies). Bacterial expression plasmids for human CapZ $\alpha$ 1 and CapZ $\beta$ 2 were generously provided by Dr. Roberto Dominguez (University of Pennsylvania, Philadelphia, PA). Human CapZ $\beta$ 2 was subcloned as a GFP fusion into the pCS2+ vector (Turner and Weintraub, 1994), whereas CapZ $\alpha$ 1 was cloned without a tag into the pCS2+ vector. A cDNA clone of mouse CARMIL1 was generously provided by Dr. Adam Zwolak (University of Pennsylvania, Philadelphia, PA). The cDNA fragment corresponding to amino acids 964–1086 of CARMIL1, which contains the region that inhibits capping protein (termed the CBR, capping-protein-binding region), was amplified by PCR and subcloned as a GFP fusion into the pCS2+ vector. The pRN3- $\beta$ -tubulin-GFP and pRN3-H2B-mCherry plasmids (McGuinness et al., 2009) were kindly provided by Dr. JungSoo Oh (Sung Kyun Kwan University, Suwon, Korea). For the GFP-FMN2 construct, a cDNA fragment corresponding to amino acids 811–1579 of mouse FMN2, which contains FH1 and FH2 domains, was amplified from cDNA isolated from MII-stage mouse oocytes and subcloned into the pCS2+ vector as a GFP fusion. cRNAs of GFP-fused mouse CapZ $\alpha$ 1 and human CapZ $\beta$ 2 were synthesized *in vitro* using the mMessage mMachine T7 Kit (Life Technologies), whereas cRNAs of GFP-fused human CapZ $\alpha$ 1 and CapZ $\beta$ 2, GFP–CARMIL<sub>CBR</sub>, GFP–FMN2,  $\beta$ -tubulin-GFP and H2B–mCherry were generated using a mMessage mMachine SP6 or T3 Kit (Life Technologies). In some cases, poly-A tails were added using a poly-A Tailing Kit (Life Technologies).

*In vitro* transcripts were purified using phenol-chloroform extraction and isopropyl alcohol precipitation and stored at –80°C until use.

### Microinjection

dsRNAs and cRNAs were microinjected into GV-stage mouse oocytes as described previously (Jang et al., 2014). To knock down capping protein, *Capza1* dsRNA and *Capzb2* dsRNA, which were diluted to 1  $\mu$ g/ $\mu$ l, were microinjected into the cytoplasm of a fully grown GV-stage oocyte using an Eppendorf Femto Jet (Eppendorf AG, Hamburg, Germany) and a Nikon Diaphot ECLIPSE TE300 inverted microscope (Nikon UK Ltd, Kingston upon Thames, Surrey, UK) equipped with a Narishige MM0-202N hydraulic three-dimensional micromanipulator (Narishige Inc., Sea Cliff, NY). After injection, oocytes were incubated in M16 medium containing 5  $\mu$ M milrinone. The oocytes were then transferred to fresh M16 medium and cultured for a further 12 h. The developmental stages of the oocytes were determined by DAPI staining. Control oocytes were microinjected with 5–10  $\mu$ l of negative control small interfering (si)RNA (Bioneer, Daejeon, Korea). Polar body extrusion and cytokinesis were observed using a stereo microscope. For rescue experiments, cRNAs encoding dsRNA-resistant human CapZ $\alpha$ 1 and GFP–CapZ $\beta$ 2 were added to the dsRNA at a concentration of 0.1  $\mu$ g/ $\mu$ l. To microinject GFP–CapZ $\beta$ 2, GFP–CARMIL<sub>CBR</sub> and GFP–FMN2 cRNAs, the concentrations of cRNA were adjusted to 1  $\mu$ g/ $\mu$ l. Approximately 5–10  $\mu$ l of cRNA was microinjected into the cytoplasm of a fully-grown GV-stage oocyte. After injection, oocytes were cultured in M16 medium containing 5  $\mu$ M milrinone, and then washed five times in fresh M16 medium for 2 min each time. The oocytes were then transferred to fresh M16 medium and cultured under paraffin oil at 37°C in an atmosphere of 5% CO<sub>2</sub> in air. Control oocytes were microinjected with 5–10  $\mu$ l of GFP cRNA.

### Immunostaining and confocal microscopy

For immunostaining of capping protein, oocytes were fixed in 4% paraformaldehyde dissolved in phosphate-buffered saline (PBS) and then transferred to a membrane permeabilization solution (0.5% Triton X-100) for 1 h. After 1 h in blocking buffer (PBS containing 1% BSA), the oocytes were incubated overnight at 4°C with a mouse anti-CapZ $\beta$ 2 antibody (Schafer et al., 1996) diluted 1:200. After three washes in washing buffer (PBS containing 0.1% Tween 20 and 0.01% Triton X-100), the oocytes were labeled with Alexa-Fluor-488-conjugated goat anti-mouse-IgG (1:100) for 1–2 h at room temperature. To stain the cytoplasmic actin mesh or cortical actin, the oocytes were fixed and stained with phalloidin-TRITC (10  $\mu$ g/ml), which labels F-actin. For anti-lectin-FITC and anti- $\alpha$ -tubulin-FITC (1:200) antibody staining, oocytes were incubated with these reagents for 1 h, washed three times in washing buffer for 2 min each time, incubated with Hoechst 33342 (10  $\mu$ g/ml in PBS) for 15 min and then washed three times in washing buffer. Samples were mounted onto glass slides and examined using a confocal laser-scanning microscope (Zeiss LSM 710 META, Jena, Germany) using a 40 $\times$  water-immersion objective lens for fixed oocytes and a 63 $\times$  oil-immersion objective lens for cytoplasmic actin mesh staining. The fluorescence intensities of CapZ $\beta$ 2 and actin labeling were quantified using ImageJ software (Schneider et al., 2012).

### Western blot analysis

A total of 100 mouse oocytes were placed in 1 $\times$  SDS sample buffer and heated at 100°C for 5 min. Proteins were separated by SDS-PAGE and transferred to polyvinylidene fluoride membranes. Thereafter, membranes were blocked in TBS-T (Tris-buffered saline containing 0.1% Tween 20) containing 5% non-fat milk for 1 h and incubated at 4°C overnight with a mouse anti-CapZ $\beta$ 2 antibody (1:1000) or a rabbit anti- $\beta$ -actin antibody (1:1000; 13E5, Cell Signaling Technology, Beverly, MA). Membranes were washed three times with TBS-T (10 min each time) and incubated at 20°C for 1 h with HRP-conjugated goat anti-mouse-IgG or anti-rabbit-IgG (1:1000; Santa Cruz Biotech, Santa Cruz Biotechnology, CA). Signals were detected using Pierce ECL western blotting substrate (Thermo Fisher Scientific, Rockford, IL).

### Time-lapse microscopy of oocyte maturation

Time-lapse imaging was performed on oocytes in which capping protein was knocked down or overexpressed. dsRNA or cRNA was microinjected into GV-stage oocytes, as described above. To visualize spindles or chromosomes,  $\alpha$ -tubulin-eGFP cRNA or H2B-mCherry mRNA was also injected. Time-lapse imaging was performed using a confocal laser scanning microscope (Zeiss LSM 710 META) equipped with a Plan Apochromat 40 $\times$  1.2 NA water-immersion objective and a Chamlide™ observation chamber and incubator system (Live Cell Instrument, Seoul, Korea). Images were captured at 300 s intervals for 7–8 h.

### Spindle and chromatin tracking

To track the spindle, single multicolor  $z$  slices were aligned based on the differential interference contrast channel to remove sample drift using a modified version of the StackRegJ plugin (Thévenaz et al., 1998) for ImageJ (Schneider et al., 2012). The centroid position of the spindle or the position of chromatin was tracked using the MTrackJ plugin (Meijering et al., 2012) for ImageJ, using the GFP or RFP channels of images processed by segmented thresholding. The distances between the centroid positions of the spindle at the starting point and at subsequent time points were recorded.

### Data analysis

For each treatment, at least three replicates were performed. Statistical analyses were conducted using Welch's  $t$ -test, Pearson's  $\chi^2$  test, Fisher's exact test or an analysis of variance (ANOVA), followed by Tukey's multiple comparisons of means by R (R Development Core Team, Vienna, Austria). Data are expressed as the mean  $\pm$  s.e.m., and  $P < 0.05$  was considered significant.

### Acknowledgements

We thank Roberto Dominguez and Adam Zwolak (Department of Physiology, University of Pennsylvania, PA) for providing the human CapZ $\alpha\beta$  and mouse CARMIL1 constructs and Tatyana Svitkina (Department of Biology, University of Pennsylvania, PA) for helpful suggestions.

### Competing interests

The authors declare no competing interests.

### Author contributions

S.N. and N.H.K. conceived the study; Y.J., W.J. and S.N. performed experiments; Y.J. and S.N. designed experiments; Y.J., S.N. and N.H.K. interpreted data; S.N. and Y.J. wrote manuscripts with comments and advices from N.H.K.

### Funding

This work was supported by grants from the Next Generation Biogreen 21 Program [grant number PJ009594] of the Rural Development Agency, Republic of Korea.

### Supplementary material

Supplementary material available online at <http://jcs.biologists.org/lookup/suppl/doi:10.1242/jcs.163576/-IDC1>

### References

- Akin, O. and Mullins, R. D. (2008). Capping protein increases the rate of actin-based motility by promoting filament nucleation by the Arp2/3 complex. *Cell* **133**, 841–851.
- Almonacid, M., Terret, M. E. and Verlhac, M. H. (2014). Actin-based spindle positioning: new insights from female gametes. *J. Cell Sci.* **127**, 477–483.
- Azoury, J., Lee, K. W., Georget, V., Rassinier, P., Leader, B. and Verlhac, M. H. (2008). Spindle positioning in mouse oocytes relies on a dynamic meshwork of actin filaments. *Curr. Biol.* **18**, 1514–1519.
- Azoury, J., Lee, K. W., Georget, V., Hikal, P. and Verlhac, M. H. (2011). Symmetry breaking in mouse oocytes requires transient F-actin meshwork destabilization. *Development* **138**, 2903–2908.
- Bamburg, J. R. and Bernstein, B. W. (2010). Roles of ADF/cofilin in actin polymerization and beyond. *F1000 Biol. Rep.* **2**, 62.
- Bear, J. E. and Gertler, F. B. (2009). Ena/VASP: towards resolving a pointed controversy at the barbed end. *J. Cell Sci.* **122**, 1947–1953.
- Bear, J. E., Svitkina, T. M., Krause, M., Schafer, D. A., Loureiro, J. J., Strasser, G. A., Maly, I. V., Chaga, O. Y., Cooper, J. A., Borisy, G. G. et al. (2002). Antagonism between Ena/VASP proteins and actin filament capping regulates fibroblast motility. *Cell* **109**, 509–521.
- Blanchoin, L., Amann, K. J., Higgs, H. N., Marchand, J. B., Kaiser, D. A. and Pollard, T. D. (2000a). Direct observation of dendritic actin filament networks nucleated by Arp2/3 complex and WASP/Scar proteins. *Nature* **404**, 1007–1011.
- Blanchoin, L., Pollard, T. D. and Mullins, R. D. (2000b). Interactions of ADF/cofilin, Arp2/3 complex, capping protein and profilin in remodeling of branched actin filament networks. *Curr. Biol.* **10**, 1273–1282.
- Caldwell, J. E., Heiss, S. G., Mermall, V. and Cooper, J. A. (1989). Effects of CapZ, an actin capping protein of muscle, on the polymerization of actin. *Biochemistry* **28**, 8506–8514.
- Chaigne, A., Campillo, C., Gov, N. S., Voituriez, R., Azoury, J., Umaña-Díaz, C., Almonacid, M., Queguiner, I., Nassoy, P., Sykes, C. et al. (2013). A soft cortex is essential for asymmetric spindle positioning in mouse oocytes. *Nat. Cell Biol.* **15**, 958–966.
- Cooper, J. A. and Pollard, T. D. (1985). Effect of capping protein on the kinetics of actin polymerization. *Biochemistry* **24**, 793–799.
- Cooper, J. A. and Sept, D. (2008). New insights into mechanism and regulation of actin capping protein. *Int. Rev. Cell Mol. Biol.* **267**, 183–206.
- Dehapiot, B., Carrière, V., Carroll, J. and Halet, G. (2013). Polarized Cdc42 activation promotes polar body protrusion and asymmetric division in mouse oocytes. *Dev. Biol.* **377**, 202–212.
- Deng, M., Suraneni, P., Schultz, R. M. and Li, R. (2007). The Ran GTPase mediates chromatin signaling to control cortical polarity during polar body extrusion in mouse oocytes. *Dev. Cell* **12**, 301–308.
- Dumont, J., Million, K., Sunderland, K., Rassinier, P., Lim, H., Leader, B. and Verlhac, M. H. (2007). Formin-2 is required for spindle migration and for the late steps of cytokinesis in mouse oocytes. *Dev. Biol.* **301**, 254–265.
- Edwards, M., Liang, Y., Kim, T. and Cooper, J. A. (2013). Physiological role of the interaction between CARMIL1 and capping protein. *Mol. Biol. Cell* **24**, 3047–3055.
- Fan, Y., Tang, X., Vitriol, E., Chen, G. and Zheng, J. Q. (2011). Actin capping protein is required for dendritic spine development and synapse formation. *J. Neurosci.* **31**, 10228–10233.
- Firat-Karalar, E. N. and Welch, M. D. (2011). New mechanisms and functions of actin nucleation. *Curr. Opin. Cell Biol.* **23**, 4–13.
- Goode, B. L. and Eck, M. J. (2007). Mechanism and function of formins in the control of actin assembly. *Annu. Rev. Biochem.* **76**, 593–627.
- Holubcová, Z., Howard, G. and Schuh, M. (2013). Vesicles modulate an actin network for asymmetric spindle positioning. *Nat. Cell Biol.* **15**, 937–947.
- Iserberg, G., Aebi, U. and Pollard, T. D. (1980). An actin-binding protein from *Acanthamoeba* regulates actin filament polymerization and interactions. *Nature* **288**, 455–459.
- Jang, W. I., Jo, Y. J., Kim, H. C., Jia, J. L., Namgoong, S. and Kim, N. H. (2014). Non-muscle tropomyosin (Tpm3) is crucial for asymmetric cell division and maintenance of cortical integrity in mouse oocytes. *Cell Cycle* **13**, 2359–2369.
- Jung, G., Remmert, K., Wu, X., Volosky, J. M. and Hammer, J. A., III (2001). The Dictyostelium CARMIL protein links capping protein and the Arp2/3 complex to type I myosins through their SH3 domains. *J. Cell Biol.* **153**, 1479–1498.
- Kim, T., Ravilious, G. E., Sept, D. and Cooper, J. A. (2012). Mechanism for CARMIL protein inhibition of heterodimeric actin-capping protein. *J. Biol. Chem.* **287**, 15251–15262.
- Kovar, D. R., Kuhn, J. R., Tichy, A. L. and Pollard, T. D. (2003). The fission yeast cytokinesis formin Cdc12p is a barbed end actin filament capping protein gated by profilin. *J. Cell Biol.* **161**, 875–887.
- Leader, B., Lim, H., Carabatsos, M. J., Harrington, A., Ecsedy, J., Pellman, D., Maas, R. and Leder, P. (2002). Formin-2, polyploidy, hypofertility and positioning of the meiotic spindle in mouse oocytes. *Nat. Cell Biol.* **4**, 921–928.
- Leblanc, J., Zhang, X., McKee, D., Wang, Z. B., Li, R., Ma, C., Sun, Q. Y. and Liu, X. J. (2011). The small GTPase Cdc42 promotes membrane protrusion during polar body emission via ARP2-nucleated actin polymerization. *Mol. Hum. Reprod.* **17**, 305–316.
- Li, R. and Albertini, D. F. (2013). The road to maturation: somatic cell interaction and self-organization of the mammalian oocyte. *Nat. Rev. Mol. Cell Biol.* **14**, 141–152.
- Li, Y. H., Kang, H., Xu, Y. N., Heo, Y. T., Cui, X. S., Kim, N. H. and Oh, J. S. (2013). Greatwall kinase is required for meiotic maturation in porcine oocytes. *Biol. Reprod.* **89**, 53.
- Livak, K. J. and Schmittgen, T. D. (2001). Analysis of relative gene expression data using real-time quantitative PCR and the 2 $^{-\Delta\Delta Ct}$  Method. *Methods* **25**, 402–408.
- Loisel, T. P., Boujemaa, R., Pantaloni, D. and Carlier, M. F. (1999). Reconstitution of actin-based motility of *Listeria* and *Shigella* using pure proteins. *Nature* **401**, 613–616.
- McGuinness, B. E., Anger, M., Kouznetsova, A., Gil-Bernabé, A. M., Helmhart, W., Kudo, N. R., Wuensche, A., Taylor, S., Hoog, C., Novak, B. et al. (2009). Regulation of APC/C activity in oocytes by a Bub1-dependent spindle assembly checkpoint. *Curr. Biol.* **19**, 369–380.
- Meijering, E., Dzubyachyk, O. and Smal, I. (2012). Methods for cell and particle tracking. *Methods Enzymol.* **504**, 183–200.
- Mejillano, M. R., Kojima, S., Applewhite, D. A., Gertler, F. B., Svitkina, T. M. and Borisy, G. G. (2004). Lamellipodial versus filopodial mode of the actin nanomachinery: pivotal role of the filament barbed end. *Cell* **118**, 363–373.
- Pappas, C. T., Bhattacharya, N., Cooper, J. A. and Gregorio, C. C. (2008). Nebulin interacts with CapZ and regulates thin filament architecture within the Z-disc. *Mol. Biol. Cell* **19**, 1837–1847.

- Pfender, S., Kuznetsov, V., Pleiser, S., Kerkhoff, E. and Schuh, M.** (2011). Spire-type actin nucleators cooperate with Formin-2 to drive asymmetric oocyte division. *Curr. Biol.* **21**, 955-960.
- Pollard, T. D. and Borisy, G. G.** (2003). Cellular motility driven by assembly and disassembly of actin filaments. *Cell* **112**, 453-465.
- Pollard, T. D. and Cooper, J. A.** (2009). Actin, a central player in cell shape and movement. *Science* **326**, 1208-1212.
- Pruyne, D., Evangelista, M., Yang, C., Bi, E., Zigmund, S., Bretscher, A. and Boone, C.** (2002). Role of formins in actin assembly: nucleation and barbed-end association. *Science* **297**, 612-615.
- Remmert, K., Olszewski, T. E., Bowers, M. B., Dimitrova, M., Ginsburg, A. and Hammer, J. A., III** (2004). CARMIL is a bona fide capping protein interactant. *J. Biol. Chem.* **279**, 3068-3077.
- Schafer, D. A., Jennings, P. B. and Cooper, J. A.** (1996). Dynamics of capping protein and actin assembly in vitro: uncapping barbed ends by polyphosphoinositides. *J. Cell Biol.* **135**, 169-179.
- Schneider, C. A., Rasband, W. S. and Eliceiri, K. W.** (2012). NIH Image to ImageJ: 25 years of image analysis. *Nat. Methods* **9**, 671-675.
- Sun, Q. Y. and Schatten, H.** (2006). Regulation of dynamic events by microfilaments during oocyte maturation and fertilization. *Reproduction* **131**, 193-205.
- Sun, S. C., Sun, Q. Y. and Kim, N. H.** (2011a). JMY is required for asymmetric division and cytokinesis in mouse oocytes. *Mol. Hum. Reprod.* **17**, 296-304.
- Sun, S. C., Wang, Z. B., Xu, Y. N., Lee, S. E., Cui, X. S. and Kim, N. H.** (2011b). Arp2/3 complex regulates asymmetric division and cytokinesis in mouse oocytes. *PLoS ONE* **6**, e18392.
- Sun, S. C., Xu, Y. N., Li, Y. H., Lee, S. E., Jin, Y. X., Cui, X. S. and Kim, N. H.** (2011c). WAVE2 regulates meiotic spindle stability, peripheral positioning and polar body emission in mouse oocytes. *Cell Cycle* **10**, 1853-1860.
- Sun, S. C., Wang, Q. L., Gao, W. W., Xu, Y. N., Liu, H. L., Cui, X. S. and Kim, N. H.** (2013). Actin nucleator Arp2/3 complex is essential for mouse preimplantation embryo development. *Reprod. Fertil. Dev.* **25**, 617-623.
- Thévenaz, P., Ruttimann, U. E. and Unser, M.** (1998). A pyramid approach to subpixel registration based on intensity. *IEEE Trans. Image Process.* **7**, 27-41.
- Turner, D. L. and Weintraub, H.** (1994). Expression of achaete-scute homolog 3 in *Xenopus* embryos converts ectodermal cells to a neural fate. *Genes Dev.* **8**, 1434-1447.
- Wang, Z. B., Jiang, Z. Z., Zhang, Q. H., Hu, M. W., Huang, L., Ou, X. H., Guo, L., Ouyang, Y. C., Hou, Y., Brakebusch, C. et al.** (2013). Specific deletion of *Cdc42* does not affect meiotic spindle organization/migration and homologous chromosome segregation but disrupts polarity establishment and cytokinesis in mouse oocytes. *Mol. Biol. Cell* **24**, 3832-3841.
- Wear, M. A. and Cooper, J. A.** (2004). Capping protein: new insights into mechanism and regulation. *Trends Biochem. Sci.* **29**, 418-428.
- Weaver, A. M., Young, M. E., Lee, W. L. and Cooper, J. A.** (2003). Integration of signals to the Arp2/3 complex. *Curr. Opin. Cell Biol.* **15**, 23-30.
- Yang, C., Pring, M., Wear, M. A., Huang, M., Cooper, J. A., Svitkina, T. M. and Zigmund, S. H.** (2005). Mammalian CARMIL inhibits actin filament capping by capping protein. *Dev. Cell* **9**, 209-221.
- Yi, K. and Li, R.** (2012). Actin cytoskeleton in cell polarity and asymmetric division during mouse oocyte maturation. *Cytoskeleton (Hoboken)* **69**, 727-737.
- Yi, K., Unruh, J. R., Deng, M., Slaughter, B. D., Rubinstein, B. and Li, R.** (2011). Dynamic maintenance of asymmetric meiotic spindle position through Arp2/3-complex-driven cytoplasmic streaming in mouse oocytes. *Nat. Cell Biol.* **13**, 1252-1258.
- Yi, K., Rubinstein, B. and Li, R.** (2013a). Symmetry breaking and polarity establishment during mouse oocyte maturation. *Philos. Trans. R. Soc. B* **368**, 20130002.
- Yi, K., Rubinstein, B., Unruh, J. R., Guo, F., Slaughter, B. D. and Li, R.** (2013b). Sequential actin-based pushing forces drive meiosis I chromosome migration and symmetry breaking in oocytes. *J. Cell Biol.* **200**, 567-576.
- Zigmund, S. H., Evangelista, M., Boone, C., Yang, C., Dar, A. C., Sicheri, F., Forkey, J. and Pring, M.** (2003). Formin leaky cap allows elongation in the presence of tight capping proteins. *Curr. Biol.* **13**, 1820-1823.
- Zwolak, A., Uruno, T., Piszczek, G., Hammer, J. A., 3rd and Tjandra, N.** (2010). Molecular basis for barbed end uncapping by CARMIL homology domain 3 of mouse CARMIL-1. *J. Biol. Chem.* **285**, 29014-29026.